Electrical and Mechanical Properties of Acrylonitrile-Butadiene-Styrene/Multiwall Carbon Nanotube Nanocomposites Prepared by Melt-Blending

Brajesh K. Singh, Prativa Kar, Nilesh K. Shrivastava, Susanta Banerjee, Bhanu B. Khatua

Materials Science Centre, Indian Institute of Technology, Kharagpur, India

Received 25 January 2011; accepted 23 May 2011
DOI 10.1002/app.34948
Published online 4 November 2011 in Wiley Online Library (wileyonlinelibrary.com).

ABSTRACT: The electrical properties in polymer/carbon nanotube (CNT) nanocomposites are governed not only by the degree of dispersion but also to a greater extent on the aspect ratio of the CNTs in the final composites. Melt-mixing of polymer and CNTs at high shear rate usually breaks the CNTS that lowers the aspect ratio of the nanotubes. Thus, homogeneous dispersion of CNTs while retaining the aspect ratio is a major challenge in melt-mixing. Here, we demonstrate a novel method that involves melt-blending of acrylonitrile-butadiene-styrene (ABS) and *in situ* polymerized polystyrene (PS)/multiwalled CNT (MWCNT) nanocomposites, to prepare electrically conducting ABS/MWCNT nanocomposites with very low CNT loading than reported. The rationale behind choosing PS/MWCNT as blending component was that ABS is reported to form miscible blend with the PS. Thus, (80/20 w/w) ABS/(PS/MWCNT) nanocomposites obtained by melt-blending showed electrical conductivity value $\approx 1.27 \times 10^{-6}$ S cm^{-1} at MWCNT loading close to 0.64 wt %, which is quite lower than previously reported value for ABS/MWCNT system prepared via solution blending. Scanning electron microscopy and differential scanning calorimetry analysis indicated the formation of homogenous and miscible blend of ABS and PS. The high temperature (100°C) storage modulus of ABS (1298 MPa) in the nanocomposites was increased to 1696 MPa in presence of 0.64 wt % of the MWCNT. © 2011 Wiley Periodicals, Inc. J Appl Polym Sci 124: 3165–3174, 2012

Key words: composites; conductivity; modulus; nanocomposites; percolation

INTRODUCTION

Plastics are widely used as insulator for electrical and electronic applications capitalizing their insulating properties due to their low concentration of free charge carriers. However, there are many cases where enhanced electrical conductivity of polymeric materials is needed. These applications refer mainly to electromagnetic interference shielding systems, radio frequency interference shielding systems, and to the dissipation of electrostatic charges from rotating and wearing members, or in the field of microelectronics. It experienced a remarkable growth during the last few decades filling the gap between the insulating polymers and the highly conductive metals. This evolution was triggered by the development of the conductive composites, where conductive fillers are incorporated in polymeric matrices. Fillers used for the preparation of conductive composites are carbon black and metal particles in various forms (grains, flakes, or fibers)[1–3] and sizes (from the nm to the mm region). But in 1991, discovery of carbon nanotubes (CNTs) by Iijima,[4] which could act as nanosized filler, has become milestone for development of conducting polymer composites. They can be either single walled (SWCNT) or multiwalled (MWCNT). Due to their special structure, CNTs show very high electrical and thermal conductivity along its axial direction. Apart from this, individual CNTs shows extremely high mechanical properties like Young modulus (about 1–2 TPa), bending strengths as high as 14.2 GPa,[5,6] stiffness and flexibility combined with high aspect ratio and large surface area.

It has become keen topic of interest of various researchers worldwide, for exploiting these excellent properties of CNTs for development of new tailored materials. Considerable amount of research on polymer/CNT nanocomposites has shown the potential of CNTs as electrically conducting filler combining with exceptionally good mechanical properties. Electrical conduction in polymer composite is due to the formation of conductive path of conductive fillers inside polymer matrix. The minimum loading of filler at which this conducting path is formed is known as percolation threshold for that polymer/filler composite. This percolation threshold is different for different matrix and filler system. It varies with shape, size, and most importantly dispersion of filler throughout the polymer matrix. Due to very high

Correspondence to: B. B. Khatua (khatuabb@matsc.iitkgp.ernet.in).

aspect ratio of CNTs, percolation threshold for polymer/CNT nanocomposite is very low in range of 0.1–2.5 wt % of CNT[7–12] for various polymer matrixes which is quite lower than particulate filler. While mixing nanosized filler in polymer, the major problem is their proper dispersion throughout the polymer system. These nanosized filler found as agglomerate due to presence of very high cohesive force between fillers. These agglomerates are major problems for dispersion of filler throughout the matrix. To exploit all desired properties of filler, this agglomeration should be broken which requires high amount of shear force. Various methods has been investigated and developed to introduce CNTs in polymer and prepare nanocomposite by researchers till now. Broadly, they can be classified in three different techniques: solution casting,[8,9] *in situ* polymerization of CNTs/monomer mixer,[10] and melt mixing of CNTs and polymer.[11–13]

In context with industrial applications of polymer-CNTs systems, melt mixing is the preferred method of composite preparation. The tendency of nanotubes to form aggregates may be minimized by appropriate application of shearing force during melt mixing. Acrylonitrile-butadiene-styrene (ABS) is widely used as engineering thermoplastics, owing to its superior chemical properties, excellent toughness, and good dimensional stability. ABS can be easily machined into products with excellent surface appearance. Due to this, ABS composites compound with other materials has been a topic of great interest. However adding, electrically conducting additives such as carbon black and CNTs to the ABS resin, the number of potential applications for this material can be further increased. ABS polymer composites, where various levels of conductivity are needed include electromagnetic shielding materials and electrically conductive composite plastic sheets useful for packaging of integrated circuit devices.[14–17] For the packaging of electronic components, antistatic features are frequently required. This is because some circuits can be damaged by static electrical charges if they are packed in insulating sheets. Oua et al.[18] prepared composites consisting of an ABS polymer matrix and a conducting carbon black (CB) additive by twin-screw extrusion and percolation threshold was found to be between 8 and 10% CB. Hom et al.[19] reported the percolation at 10 wt % CB in melt-mixed polypropylene (PP)/ABS and carbon black composites. Bose et al.[20] found the percolation threshold at $\sim$ 3–4 wt % MWCNT in melt-mixed co-continuous blends of polyamide 6 (PA6) and ABS using MWCNT. Wang et al.[21] have prepared composites of ABS/MWCNTs via solution-blending. The MWCNT-filled ABS shows percolation point of the electrical conductivity at filler loadings of $\sim$ 1–2 wt %.

In summary, literature on ABS/CNT nanocomposites, prepared by various methods, reports that the percolation threshold of CNT in the nanocomposites is above 1 wt % of CNT loading. Here, we introduce a novel technique for the preparation of electrically conductive ABS/MWCNT nanocomposites at very low CNT loading than ever reported, which involves melt-mixing of ABS and *in situ* polymerized PS/MWCNT nanocomposites. The reason behind blending PS/MWCNT with ABS is that PS forms miscible blend with ABS. Thus, predispersed CNTs in PS were dispersed in the ABS matrix through melt blending PS/MWCNT with ABS. Effect of PS on storage modulus of the nanocomposite is also investigated with variation of temperature.

EXPERIMENTAL

Material and composite preparation

ABS (Toyolac 700), a copolymer of acrylonitrile (23%), butadiene (13%), and styrene (64%) was obtained from Toray Industries, Japan. This general purpose grade ABS has a molecular weight (M_w) of 13,000 and a melt flow index of 23 g/10 min at 220°C. Multiwall carbon nanotube (MWNT, NC7000) used in this study was obtained from Nanocyl SA, Belgium. Purity of the pristine MWCNTs as received was 95%. No further modification was done on the MWCNT. Styrene monomer was supplied by Merck Germany.

First, masterbatch of MWCNT was prepared in polystyrene (PS) matrix by *in situ* polymerization technique. Styrene was washed with 5% NaOH solution followed by distilled water for removing stabilizers and dried over anhydrous $MgSO_4$. The MWCNT was added in purified styrene monomer. The styrene/MWCNT mixture was ultrasonicated to break the agglomerates of CNTs and achieve good dispersion of MWCNT by using an ultrasonic generator (frequency of 28 kHz, with a power of 600 W) for 45 min at room temperature. *In situ* bulk polymerization of styrene/MWCNT was done using benzoyl peroxide as an initiator in glass reactor at 85°C for 3 h under nitrogen atmosphere. The PS/MWCNT masterbatch thus obtained had CNT loading 3.25 wt % as was calculated from the feed composition. This masterbatch at different weight ratio was melt-mixed with ABS to prepare ABS/MWCNT nanocomposites in internal mixer at 220°C and 50 rpm for 20 min. For comparative study, ABS/PS and ABS/MWCNT (1 wt %) nanocomposites was also prepared by direct melt blending at 220°C, 50 rpm for 20 min. Finally, the melt-blended nanocomposites were compression molded at 220°C under constant pressure (10 MPa) for further characterizations.

CHARACTERIZATIONS

Electrical conductivity

The direct current (DC) conductive measurements were done on the molded specimen bars of dimensions 30 × 10 × 3 mm. The sample was fractured at two ends, and the fractured surface was coated with silver paste to ensure good contact of the sample surface with electrodes. The electrical conductivities of the conducting composite were measured with a two-probe technique. The specimens were prepared under similar conditions to avoid the influence of the processing parameters on the electrical properties. Minimum of five tests were performed for each specimen, and the data was averaged.

Ac electrical conductivity and dielectric properties of the composite were obtained using a computer-controlled precision impedance analyzer (Agilent 4294A) on application of an alternating electric field across the sample cell in the frequency range of 40 Hz–10 MHz. The parameters like dielectric permittivity (ε') and dielectric loss tangent (tan δ) were obtained as a function of frequency. The alternative current (AC) conductivity (σ_{ac}) was calculated from the dielectric data using the relation:

$$\sigma_{ac} \approx \omega \varepsilon_0 \varepsilon' \tan\delta \quad (1)$$

where ω is equal to $2\pi f$ (f is the frequency), and ε_0 is vacuum permittivity. The dielectric permittivity (ε') was determined with the following equation:

$$\varepsilon' \approx \frac{C_p}{C_0} \quad (2)$$

where C_p is the observed capacitance of the sample (in parallel mode), and C_0 is the capacitance of the cell. The value of C_0 was calculated using the area (A) and thickness (d) of the sample, following the relation:

$$C_0 \approx \frac{\varepsilon_0 A}{d} \quad (3)$$

Scanning electron microscopy study

Morphological features including the state of dispersion of MWCNT in the blends were studied by scanning electron microscopy (SEM). Compression molded samples were cryofractured in liquid nitrogen. Then the fracture surface of the samples was coated with a thin layer of gold to prevent charging. These samples were then observed under SEM (VEGA II LSU, TESCAN, Czech Republic). SEM micrographs were taken at an operating voltage of 5 kV. The phase morphology of the ABS nanocomposite was studied with a field emission scanning electron microscope (Carl Zeiss-SUPRA^{TM} 40), operated at an accelerating voltage of 10 kV.

TEM analysis

The morphology of the samples was examined through high resolution transmission electron microscopy (HRTEM, JEM 2100, JEOL, Japan) at 200 kV. Ultra thin sections were prepared using Leica ultramicrotome Microsystems for TEM analysis at cryogenic condition with a thickness of 60–80 nm.

Dynamic mechanical analysis

Dynamic modulus of the composites was measured by a dynamic mechanical analyzer (DMA 2980 model). The measurements were obtained in cantilever beam mode at a constant vibration frequency of 1 Hz, temperature range of 30–180°C at a heating rate of 5°C/min, in nitrogen atmosphere. The dimension of the specimen was 30 × 6.40 × 0.45 mm^3.

Differential scanning calorimetry study

The glass transition temperature (T_g) were determined with differential scanning calorimetry (DSC-200 PC, NETZSCH, Germany). DSC analysis was performed in isothermal conditions using 5–10 mg of sample at a scanning rate of 10°C/min, under nitrogen atmosphere. The samples were heated to 250°C, held for 5 min for removing moisture and previous thermal history and then cooled to room temperature at a cooling rate of 10°C/min. The second heating scans were used for determination of glass transition temperature (T_g) of the samples.

Thermo gravimetric analysis

The nanocomposites were subjected to thermo gravimetric analysis (TGA), to analyze the effect of MWCNT loading on the thermal stability of the matrix polymer ABS, by using (Perkin Elmer Pyris Diamond TG-DTA, USA) instrument. Samples of approximately 10 mg were heated from 40°C to 600°C at a heating rate of 20°C/min in air atmosphere. The initial degradation temperature, weight loss, and final degradation temperature of the samples were recorded.

RESULTS AND DISCUSSION

Electrical properties

The resistivity of ABS/MWCNT nanocomposite with various weight content of MWCNT (p), measured at ambient temperature (30°C), is shown in Figure 1. The bulk conductivity of the ABS was increased

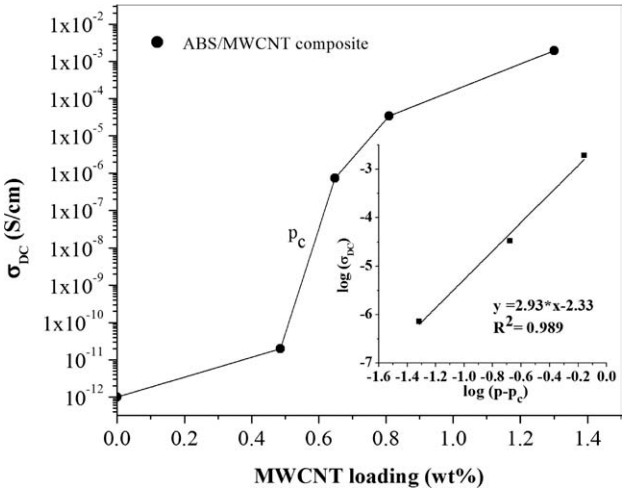

Figure 1 Dependence of the DC conductivity on the CNTs loading (p). The percolation threshold p_c is about 0.6 wt %. The inset shows the percolation scaling law between log σ_{DC} and log ($p - p_c$), where the solid line corresponds to the best fitted line.

with increasing loading of MWCNT. An abrupt percolation threshold p_c of the dc conductivity was observed at 0.6 wt % MWCNTs, indicating the existence of a percolating path via connecting the CNTs. At this stage, the conductivity of the composite is controlled by the conducting MWCNTs. The dc conductivity is due to the formation of a continuous network of MWCNTs within the polymer matrix. The highly dispersed high aspect ratio MWCNTs in the ABS matrix allow achieving the percolation at very low weight fraction of the nanotubes.

The bulk electrical conductivity of the composites with conducting filler above the percolation threshold p_c can be related with universal law via equation:

$$\sigma_{DC} \approx \sigma_0(p - p_c)^t \text{ for } p > p_c \quad (4)$$

where σ_{DC} is the conductivity of the composite with different filler content, σ_0 is the conductivity of the filler, p is the weight fraction of the filler, and p_c is critical volume fraction of the filler (percolation threshold), and t is the critical exponent.[22] The data are fitted to the scaling law, and the best-fitted values are for $p_c \sim 0.6$ wt %, $\sigma_0 \sim 4.67 \times 10^{-3}$ S/cm, and $t = 2.94 \pm 0.22$. As mentioned previously, extrapolation of $p \sim 100\%$ using eq. (4) gives a conductivity of $\sigma_0 \sim 4.67 \times 10^{-3}$ S/cm, which is 4 orders of magnitude lower than the conductivity measured in bundles of MWNTs. This has also been observed in PmPV/MWNTs,[23] PMMA/MWNTs[24] composite thin films, and epoxy/SWCNT.[25] Kilbride et al.[23] believed that such discrepancy in the conductivity values was due to a coating of the individual nanotubes by a polymer insulating surface, which resulted poor electrical contact between nanotubes. Stephan et al.[24] suggested that large contact resistances could also induce a further limitation of the conductivity to explain their low value (10^{-5} S/cm) for 16 wt % of MWCNTs in PMMA matrix. Exponent "t" value between 1.1 and 1.3 indicates the conduction through 2D network whereas for 3D network the value lies in the range of 1.6–2.[26,27] In this case, the exponent "t" value is observed to be 2.94 ± 0.22. Clearly, ABS/MWCNT blend deviates from the universal law. Such discrepancy in the exponent value was reported earlier in case of composites with carbon black.[28] Kogut and Straley[29] showed, in computer simulations, that if the low-conductance bonds in the percolation network, or the inter-granular conductance of the conducting component in a continuous system, have a very wide distribution, then t can be larger than 2. This distribution can be due to a large range of effective geometrical resistivity factors in a continuous homogeneous conducting phase.

A general relationship between the percolation threshold of systems of various objects and their associated excluded volume has been discussed by Balberg et al.[30] In the isotropic case of randomly long sticks (length L and radius R), the proposed relation is:

$$(L/R)f_c \sim 3 \quad (5)$$

where, f_c is the critical volume fraction of the stick. Assuming the stick is a bundle of CNTs and using eq. (2) and $f_c \sim 0.36$ vol %, and having $L/R \sim 850$, which is in agreement with conduction through long sticks, i.e., the MWCNTs bundles. McLachlan and Sauti[31] have shown f_c as function of aspect ratio (L/D) of random long sticks bundles and SWCNT. It can be observed form plot that f_c is inversely proportional to the aspect ratio of the sticks. Considering MWCNTs as random long stick bundle, from the graph we found that critical volume fraction (percolation) is around 0.004 for aspect ratio (L/D) of 400. The obtained $f_c \sim 0.0036$ and $L/R \sim 850$ show good agreement with that graph for percolation in the composite.

Figure 2 shows AC conductivity of ABS/MWCNT nanocomposites at various MWCNTs loading with the variation of frequency from 40 Hz to 10 MHz at 30°C. AC conductivity was increased with MWCNT weight content throughout the frequency region. In the low frequency edge, an abrupt increase of conductivity (up to eight orders of magnitude) is observed, between the nanocomposites with 0.50 and 0.65 wt % in MWCNT. This pronounced alteration is a firsthand indication that percolation threshold has been exceeded. It can be clearly observed from the plot percolation threshold p_c lies in

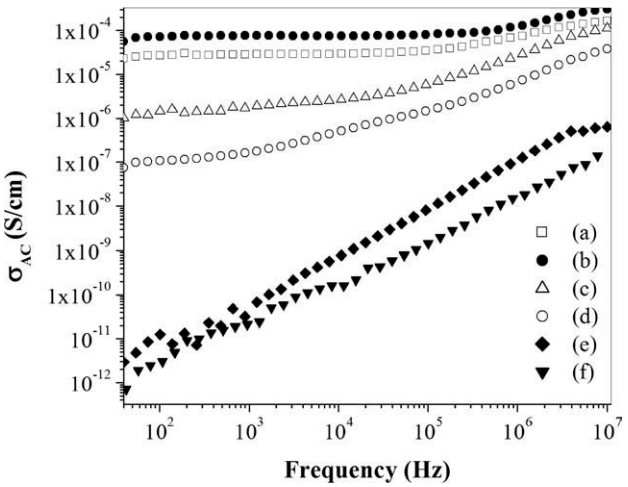

Figure 2 Frequency dependence of the of the AC conductivity for different CNT weight fraction p at 30°C: (a) melt blended ABS/CNT (1 wt %), (b) (60/40 w/w) ABS/(PS/MWCNT) with 1.30 wt % of CNT, (c) (75/25 w/w) ABS/(PS/MWCNT) with 0.81 wt % of CNT, (d) (80/20 w/w) ABS/(PS/MWCNT) with 0.65 wt % of CNT, (e) (85/15 w/w) ABS/(PS/MWCNT) with 0.50 wt % of CNT, and (f) ABS.

between 0.5 and 0.65 wt % of filler loading. Conductivity spectra for the nanocomposites with MWCNT content equal or higher than 0.65 wt % exhibited a wider plateau of the so-called apparent DC conductivity, and a narrower range where conductivity values were frequency dependent. Moreover, the frequency region of constant conductivity extends to higher frequencies with increasing weight fraction of MWCNTs. The frequency dependence of the AC conductivity follows a power law behavior, $\sigma(\omega)$ or the total AC conductivity can be then represented by the following equation:

$$\sigma(w) \approx \sigma(0) + \sigma_{AC}(\omega) \approx \sigma_{DC} + A\omega^s \qquad (6)$$

where $\omega = 2\pi f$ is the angular frequency, σ_{DC} is the independent frequency conductivity or dc conductivity (at $\omega \rightarrow 0$), A is the constant dependent on temperature T, and s is an exponent dependent on both frequency and temperature with values in the range 0–1. This type of behavior was noted by Jonscher,[32] who called it the "universal dynamic response" because of a wide variety of materials that displayed such behavior. The value of σ_{DC} can also be estimated from the plateau values of conductivity in the plot between $\sigma_{AC}(\omega)$ and ω. There exists for each composition a critical frequency ω beyond which a power law is followed. The value of DC conductivity obtained through above eq. (6) shows comparable result with respect to the measured value of DC conductivity.

Connor et al.[33] have reported in their investigations of conductor-polymer composites that the shapes of the conductivity curves were independent of conductor particles content p, and only the dc conductivity and critical frequency ω_c depend on p^2.They construct a p-independent master curve of the normalized conductivity, $\sigma_{AC}(\omega)/\sigma_{DC}$, as a function of frequency and shift factor depending on p. In Figure 3, the scaled frequency of the real part of the complex conductivity for $p \geq p_c$ is shown. By plotting $\sigma_{AC}(\omega)/\sigma_{DC}$ vs. $a_p\ \omega$ the conductivity data fall on almost one single curve showing good agreement to their report, where a_p is the shift factor defined as:

$$a_p \approx \omega_c(\text{ref})/\omega_c \qquad (7)$$

Here the reference content was 1.3 wt % with $\omega_c(\text{ref}) = 3.29 \times 10^5\ \text{s}^{-1}$ and ω_c is corresponding critical frequency for each composite having loading above percolation threshold. Values of ω_c measured were 3.64×10^2, 1.10×10^4, and $9.47 \times 10^4\ \text{s}^{-1}$ for 0.65, 0.75, and 1.00 wt % of CNT loading, respectively.

Dielectric properties of the nanocomposite were also investigated. Increase in dielectric properties like dielectric constant (ε') and dielectric loss (ε'') with increase in filler loading was observed. Figures 4 and 5 show dielectric constant (ε') and dielectric loss (ε'') with variation of frequency, respectively. The curves can be distinguished between the two groups. The composites with 0.5 wt % MWCNTs and pure ABS had a nearly constant ε' value, with only small changes in ε''. However, composites with MWCNTs loading higher than 0.65 wt

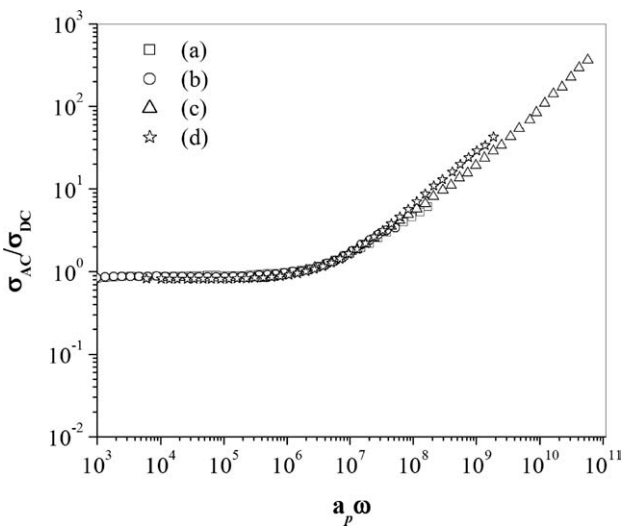

Figure 3 Master curve plotted $\sigma_{AC}(\omega)/\sigma_{DC}$ as a function of frequency and shift factor ($a_p\ \omega$) for $p \geq p_c$: (a) melt blended ABS/CNT (1 wt %), (b) (60/40 w/w) ABS/(PS/MWCNT) with 1.30 wt % of CNT, (c) (75/25 w/w) ABS/(PS/MWCNT) with 0.81 wt % of CNT, and (d) (80/20 w/w) ABS/(PS/MWCNT) with 0.65 wt % of CNT.

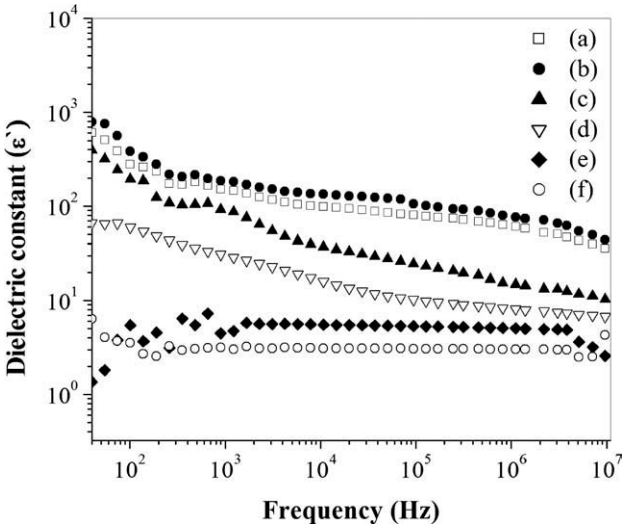

Figure 4 Dielectric constant as function of frequency (Hz): (a) melt blended ABS/CNT (1 wt %), (b) (60/40 w/w) ABS/(PS/MWCNT) with 1.30 wt % of CNT, (c) (75/25 w/w) ABS/(PS/MWCNT) with 0.81 wt % of CNT, (d) (80/20 w/w) ABS/(PS/MWCNT) with 0.65 wt % of CNT, (e) (85/15 w/w) ABS/(PS/MWCNT) with 0.50 wt % of CNT, and (f) ABS.

% showed a significantly high increment in dielectric constant. The dielectric constant (permittivity) increased because of space charge built up at the interfaces between the polymer phase and the added conducting filler (MWCNT) phase due to their difference in the conductivity. Space charge polarization occurs when more than one material component is present or when segregation occurs in a material containing incompatible chemical sequences. Due to this, translating charge carriers become trapped at the interfaces of these heterogeneous systems and the electric field distortion caused by these accumulated charges increases the overall capacitance of a material, which appears as an increase in the dielectric constant. Near percolation, this phenomenon is more prominent. Above percolation, composite is conducting due to formation of conducting path in matrix which should lead to decrease in space charge built up and hence decrease in dielectric. However, in ABS/(PS/MWCNT) nanocomposites, the dielectric constant was increased above the percolation (0.6 wt %) of MWCNT. Such behavior has been reported earlier for polymer composites containing carbon black[26,34] and was attributed to "micro capacitors" remaining in the sample above p_c. These "micro capacitors" are assumed to be formed by gaps between MWCNTs in polymer matrix. The value of ε' and ε'' was decreased with increasing the frequency. The decrease in the dielectric constant with increase in frequency is explained by the fact that, in higher frequency range, the interfacial dipoles have less time to orient themselves in the direction of the alternating field.

Dielectric losses exhibited high values and formed in the low frequency range. When the frequency was increased, the dielectric loss decreased quickly. As the content of MWCNT is increased, the higher filler content increases the heterogeneity of the system, produces extended interfaces, and results in increased conductivity and higher losses. Electron transport through MWCNT might be responsible for the accumulation of charges at the interfaces, and the large leakage current in the low frequency range.

Morphological studies

Surface morphology of the composite was investigated through SEM. For further detail of morphology, FESEM analysis is also done. Figure 6 shows the images of (75/25 w/w) ABS/(PS/MWCNT) nanocomposites with 0.81 wt % CNT. From SEM micrographs, it can be clearly seen that no phase separation exists between ABS and PS, indicating the formation of miscible blend. White spherical domains appearing in image are rubbery phase consists of poly(butadiene) molecule, dispersed throughout the matrix. Formation of continuous network like structure in the nanocomposites due to MWCNT is observed in Figure 6(b). Exploring further for network structure, FESEM micrograph is investigated. Figure 6(c,d) confirm the network structure and presence of MWCNT are clearly visible. Formation of network like structure confirms the formation of conducting path and attainment to percolation threshold value. Appearance of small voids in

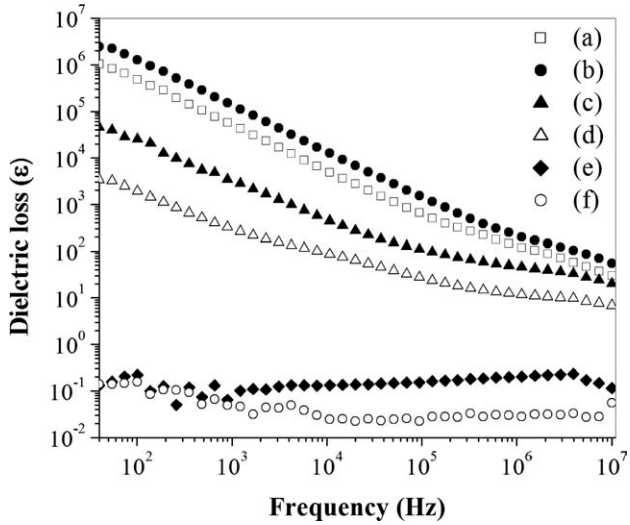

Figure 5 Dielectric loss as function of frequency (Hz): (a) melt blended ABS/CNT (1 wt %), (b) (60/40 w/w) ABS/(PS/MWCNT) with 1.30 wt % of CNT, (c) (75/25 w/w) ABS/(PS/MWCNT) with 0.81 wt % of CNT, (d) (80/20 w/w) ABS/(PS/MWCNT) with 0.65 wt % of CNT, (e) (85/15 w/w) ABS/(PS/MWCNT) with 0.50 wt % of CNT, and (f) ABS.

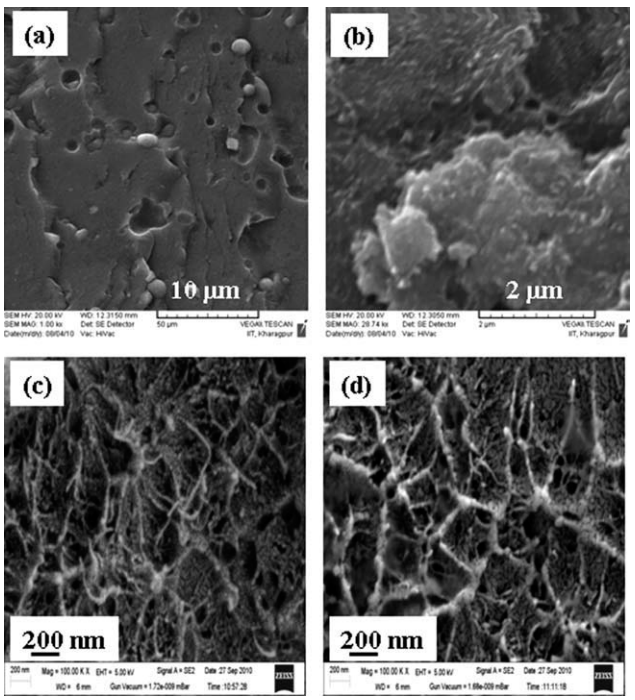

Figure 6 (a, b) SEM micrographs and (c, d) FESEM micrographs of nanocomposite (75/25 w/w) ABS/(PS/MWCNT) with 0.81 wt % of CNT.

images [Fig. 6(c,d)] at very high magnification (100 kX) indicated poor interfacial adhesion between the matrix polymers and MWCNT in the nanocomposites. Further increase in MWCNT loading does not affect morphology of composites significantly, but there is increment in concentration of network structure in the matrix.

Bulk property of composite was seen through transmission electron microscopy (TEM). Figure 7 shows TEM image of the (75/25 w/w) ABS/(PS/MWCNT) nanocomposites with 0.81 wt % CNT. Images of Figure 7(a,b) were taken at 12k magnification whereas Figure 7(c,d) were taken at 20k and 30k magnification, respectively, at different locations. All TEM images show good dispersion of MWCNT throughout the matrix. Dark small circle are the end of MWCNT which were cut during sample preparation. In Figure 7(b), the presence of dark particle is due to the rubbery phase of ABS. Li and Shimizu[35] prepared polyamide6/ABS cocontinuous blends and observed the black particles in TEM microgarph which were attributed to the butadiene rubber phase having diameter around 200 nm. Piorkowska et al.[36] had also found polybutadiene (rubbery) domain in TEM image of similar diameter in blend of PS/ABS.

Dynamic mechanical property

Dynamic mechanical analysis measures the viscoelastic properties of polymers under stress and elevated temperature. Figure 8 shows the variation in storage modulus and tan δ with temperature changes from 30°C to 150°C for pure ABS and its MWCNT nanocomposites (the left axis represents variation of storage modulus and the right axis represents variation of dissipation factor of the nanocomposites). At the lower temperature region (<70°C), pure ABS shows lowest storage modulus (∼ 1500 MPa). (80/20 w/w) ABS/(PS/MWCNT) nanocomposites [Fig. 8(b)] shows significant increase

Figure 7 TEM micrographs of nanocomposite (75/25 w/w) ABS/(PS/MWCNT) with 0.81 wt % of CNT at different magnifications; (a, b) at 12k, (c) 20k, and (d) 30k magnification.

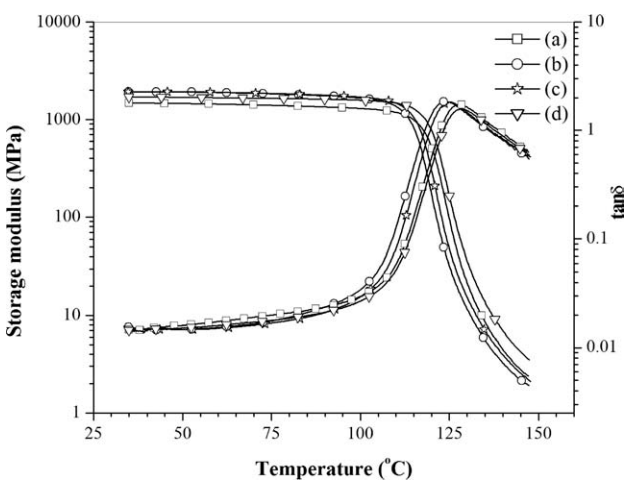

Figure 8 Storage modulus and loss tangent curves of pure ABS and the composites with different composition and filler content: (a) ABS, (b) (80/20 w/w) ABS/PS, (c) (80/20 w/w) ABS/(PS/MWCNT) with 0.65 wt % of CNT, and (d) melt blended ABS/CNT (1 wt %).

TABLE I
Dynamic Mechanical Property of ABS/MWCNT Composites

Sample	E' (MPa) at different temperatures			T_g	tan
	50°C	100°C	120°C	(°C)	δ_{max}
ABS	1460	1298	612	127	1.72
(80/20 w/w) ABS/PS	1913	1653	180	125	1.82
(80/20 w/w) ABS/(PS/MWCNT) with 0.65 wt % of CNT	1928	1696	442	124	1.84
ABS/CNT (1 wt %)	1680	1575	814	128	1.55

in storage modulus. From plot, it can be observed that addition of MWCNT to the composite [Fig. 8(c)] leads to maximum value storage modulus. So, it can be assumed form the plot major increment in storage modulus is due to the incorporation of PS only (as nanocomposite ABS/CNT (1 wt %) show intermediate storage modulus value) and MWCNT further enhances the storage modulus value. These evident improvements could be attributed to incorporation of stiff PS molecule (increases the stiffness of molecule) and MWCNT interfacial adhesion with the ABS matrix, which reduces chain mobility of the polymer in the interfacial region and enhances the stiffening properties of the composites. The modulus (ε') at different temperatures and tan δ_{max} values are shown in Table I.

At higher temperature (above 70°C), fall in mechanical property is evident which is more prominent for PS mixed composite due to chain movement of lower molecular weight PS. It shows that PS decreases thermal stability of the composite. At around 110°C, sudden drop in storage modulus was observed. However, composite having MWCNT shows higher thermal stability than other, and ABS/CNT (1 wt %) nanocomposites shows highest thermal stability. It can be due to network structure formation which restricts the flow of polymer chain and improve high temperature storage modulus.

It is well known that the temperature corresponding to the maximum of a tan δ peak is well associated with the glass transition temperature (T_g) of the concerned material. The tan δ peak at ~ 128°C for pure ABS indicates the T_g ABS (Fig. 8). However, a slight decrease in T_g (124°C) is evident in (80/20 w/w) ABS/PS blend. This reduction of glass transition temperature of ABS in the blend is the result of mixing low molecular weight PS with ABS. Presence of 0.65 wt % MWCNT in (80/20 w/w) ABS/(PS/MWCNT) does not increases the T_g of the (80/20 w/w) ABS/PS blend.

Thermal property

Figure 9 shows the DSC thermogram of ABS and their various composites. A sharp dip along with a small dip in base line is observed around ~ 106°C which signifies T_g of pure ABS. Jang et al.[37] also observed the same type of thermogram for ABS and suggested that it could be due to non homogeneous nature of copolymer. We assumed that it could be due to acrylonitrile component of ABS which shows small extent of crystallization due to polar nature of nitrile (C≡N) group.

It could also be observed that with addition of *in situ* polymerized PS/MWCNT masterbatch in the ABS, the DSC heating scan became smoothening in nature. As evident from the thermograms, incorporation of PS slightly lowers the T_g value (≈102°C) of ABS in (80/20 w/w) ABS/PS blend. This is due to the presence of molecular weight PS (lower T_g than ABS), which forms miscible ABS/PS blend and thus the T_g of the blend is appeared at lower temperature. In the ABS/(PS/MWCNT) nanocomposites with various CNT content (0.5–0.81 wt %), the T_g of ABS appears at a temperature almost similar to that of (80/20 w/w) ABS/PS blend. However, a marginal increase (≈107°C) in T_g of the blend is evident at higher loading (1.3 wt %) of MWCNT in the nanocomposites. Moreover, the T_g of melt blended ABS/MWCNT (1 wt %) nanocomposites appears at ≈106°C, very close to the T_g of pure ABS. These results indicate that T_g of ABS remains unaffected in presence of small amount of MWCNT in the nanocomposites.

The degradation pattern of the pure ABS and ABS/MWCNT composites in air was analyzed and shown in Figure 10. TGA curve shows same pattern

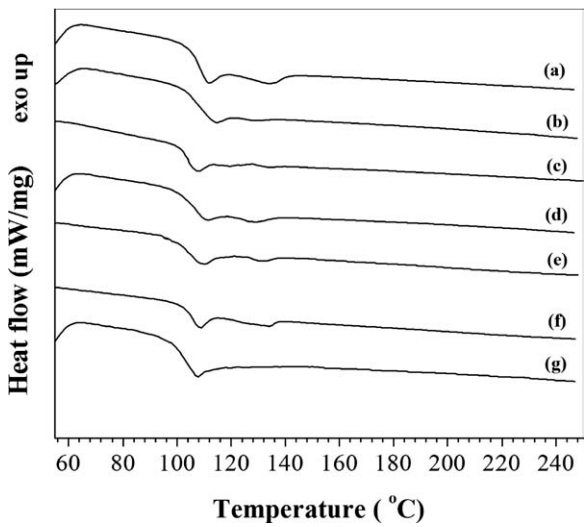

Figure 9 DSC thermogram of ABS nanocomposites: (a) melt blended ABS/CNT (1 wt %), (b) (60/40 w/w) ABS/(PS/MWCNT) with 1.30 wt % of CNT, (c) (75/25 w/w) ABS/(PS/MWCNT) with 0.81 wt % of CNT, (d) (80/20 w/w) ABS/(PS/MWCNT) with 0.65 wt % of CNT, (e) (85/15 w/w) ABS/(PS/MWCNT) with 0.50 wt % of CNT, (f) ABS, and (g) (80/20 w/w) ABS/PS.

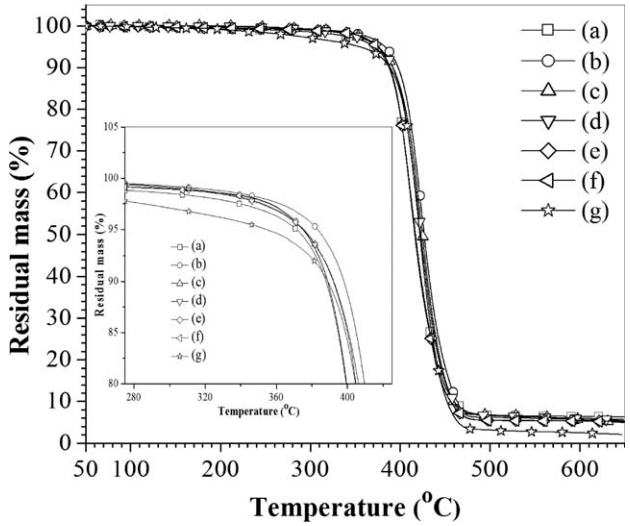

Figure 10 TGA thermogram of ABS nanocomposites: (a) melt blended ABS/CNT (1 wt %), (b) (60/40 w/w) ABS/(PS/MWCNT) with 1.30 wt % of CNT, (c) (75/25 w/w) ABS/(PS/MWCNT) with 0.81 wt % of CNT, (d) (80/20 w/w) ABS/(PS/MWCNT) with 0.65 wt % of CNT, (e) (85/15 w/w) ABS/(PS/MWCNT) with 0.50 wt % of CNT, (f) ABS, and (g) (80/20 w/w) ABS/PS.

of degradation for almost all the composites. ABS/MWCNT composite showed higher thermal stability, and the initial degradation started above 250°C and completed at 480°C. Comparing thermogram of pure ABS and ABS/CNT (1 wt %), an interesting fact was observed in degradation pattern of the nanocomposite. At temperature below 440°C, rate of degradation for ABS/CNT (1 wt %) composite was higher than pure ABS, and above 440°C, its degradation rate became slow than the pure ABS. This signifies that MWCNTs reduce thermal stability of ABS at lower temperature, but above 440°C, it stabilizes the decomposition of ABS. Same type of phenomenon was observed and reported by other researcher.[21,38] Again, (80/20 w/w) ABS/(PS/MWCNT) showed lower thermal stability than ABS where degradation started at much lower temperature (~ 150°C) and completed at 480°C. It is due to the presence of low molecular weight PS in ABS matrix. (85/15 w/w) ABS/(PS/MWCNT) blend with 0.5 wt % MWCNT also showed thermal stability almost similar to pure ABS, but all other composite (80/20 w/w) ABS/(PS/MWCNT) with 0.65 wt % of CNT, (75/25 w/w) ABS/(PS/MWCNT) with 0.81 wt % of CNT, and (60/40 w/w) ABS/(PS/MWCNT) with 1.30 wt % of CNT had shown higher thermal stability than pure ABS. Composite having higher wt % of CNT sustained much temperature and its degradation started at later stage. (60/40 w/w) ABS/(PS/MWCNT) blend with 1.3 wt % MWCNT showed highest thermal stability. Interestingly, it could be seen that MWCNT as well as PS both were decreasing the thermal stability of composite when present alone with ABS in the matrix. But, when used together they showed synergistic property and enhanced the thermal stability of the nanocomposites.

CONCLUSION

Nanocomposite of ABS and MWCNT has been prepared by melt-mixing of ABS and PS/MWCNT masterbatch. A good dispersion of CNT was achieved throughout the ABS matrix by melt-blending of ABS with predispersed MWCNTs in PS matrix. The electric conductivity measurement revealed the electrical percolation threshold at around ~ 0.60 wt % of MWCNT in ABS matrix. Improvement in dielectric properties of ABS was also observed by 3 orders of magnitude in the nanocomposites. DMA result confirmed the stiffening effect of MWCNT that increased the storage modulus of the nanocomposites. DSC study revealed that T_g of ABS was not affected in the presence of lower loading of MWCNT in the nanocomposites. TGA thermograms showed that presence of MWCNTs tend to destabilize the thermal stability of nanocomposite in the 250–440°C temperature range but improved slightly above 440–650°C temperature range. Synergistic effect is also shown by the MWCNTs and PS on thermal stability of the nanocomposite. Higher thermal stability of ABS/MWCNT nanocomposite was achieved through this method.

References

1. Gubbels, F.; Jerome, R.; Teyssie, P.; Vanlathem, E.; Deltour, R.; Calderone, A.; Parente, V.; Bredas, J. L. Macromolecules 1994, 27, 1972.
2. Boudenne, A.; Ibos, L.; Fois, M.; Gehin, E.; Majeste, J. C. J Polym Sci Part B: Polym Phys 2004, 42, 722.
3. Naebe, M.; Hurren, C.; Maazouz, A.; Lamnawar, K.; Wang, X. Fibers Polym 2009, 10, 662.
4. Iijima, S. Nature 1991, 345, 56.
5. Wong, E. W.; Sheehan, P. E.; Lieber, C. M. Science 1997, 277, 1971.
6. Treacy, M. M. J.; Ebbesen, T. W.; Gibson, J. M. Nature 1996, 381, 678.
7. Wang, Z.; Lu, M.; Lia, H. L.; Guo, X. Y. Mater Chem Phys 2006, 100, 77.
8. Sun, G.; Chen, G.; Liu, Z.; Chen, M. Carbon 2010, 48, 1434.
9. Bhatia, R.; Prasad, V.; Menon, R. Mater Sci Eng B 2010, 175, 189.
10. Kim, S. T.; Choi, H. J.; Hong, S. M. Colloid Polym Sci 2007, 285, 593.
11. Haggenmuller, R.; Gonmas, H. H.; Rinzler, A. G.; Fischer, J. E.; Winey, K. I. Chem Phys Lett 2000, 330, 219.
12. Abbasi, S.; Carreau, P. J.; Derdouri, A.; Moan, M. Rheol Acta 2009, 48, 943.
13. Kasaliwal, G.; Göldel, A.; Pötschke, P. J Appl Polym Sci 2009, 112, 3494.
14. Ma, C. C.; Hu, A. T.; Chen, D. K. Polym Polym Compos 1993, 1, 93.
15. Lu, G.; Li, X.; Jiang, H.; Mao, X. J Appl Polym Sci 1996, 62, 2193.

16. Yonezawa, M. Jpn. Pat. JP 08039734 (1996).
17. Myagawa, K.; Shimizu, M.; Inoe, M. Jpn. Pat. JP 06305084 (1994).
18. Oua, R.; Gerhardta, R. A.; Marrett, C.; Moulart, A.; Colton, J. S. Compos Part B 2003, 34, 607.
19. Hom, S.; Bhattacharyya, A. R.; Khare, R. A.; Kulkarni, A. R.; Saroop, M.; Biswas, A. J Appl Polym Sci 2009, 112, 998.
20. Bose, S.; Bhattacharyya, A. R.; Kulkarni, A. R.; Pötschke, P. Compos Sci Technol 2009, 69, 365.
21. Wang, W.; Luo, G.; Wei, F.; Luo, J. Polym Eng Sci 2009, 49, 2144.
22. Stauffer, G. Introduction to Percolation Theory; Taylor & Francis: London, 1985
23. Kilbride, B. E.; Coleman, J. N.; Fraysse, J.; Fournet, P.; Cadek, M.; Drury, A.; Hutzler, S.; Roth, S.; Blau, W. J. J Appl Phys 2002, 92, 4024.
24. Stephan, C.; Thien Phap, N.; Lahr, B.; Blau, W.; Lefrant, S.; Chauvet, O. J Mater Res 2002, 17, 396.
25. Barrau, S.; Demont, P.; Peigney, A.; Laurent, C.; Lacabanne, C. Macromolecules 2003, 36, 5187.
26. Pötschke, P.; Dudkin, S. M.; Alig, I. Polymer 2003, 44, 5023.
27. Dai, K.; Xu, X. B.; Li, Z. M. Polymer 2007, 48, 849.
28. Calberg, C.; Blacher, S.; Gubbels, F.; Brouers, F.; Deltour, R.; Jěrŏme, R. J. Phys D: Appl Phys 1999, 32, 1517.
29. Kogut, P. M.; Straley, J. P. J Phys C: Solid State Phys 1979, 12, 2151.
30. Balberg, I.; Anderson, C. H.; Alexander, S.; Wagner, N. Phys Rev B 1984, 30, 3933.
31. McLachlan, D. S.; Sauti, G. J Nanomater 2007, 2007, 30389.
32. Jonscher, A. K. Nature (London) 1977, 267, 673.
33. Connor, M. T.; Roy, S.; Ezquerra, T. A.; Balta, C. J. Phys Rev B 1998, 57, 2286.
34. McLachlan, D. S.; Heaney, M. B. Phys Rev B 1999, 60, 12746.
35. Li, Y.; Shimizu, H. Macromol Rapid Commun 2005, 26, 710.
36. Piorkowska, E.; Argon, A. S.; Cohen, R. E. Polymer 1993, 34, 4435.
37. Jang, L. W.; Kang, C. M.; Lee, D. C. J Polym Sci Part B: Polym Phys 2001, 39, 719.
38. Yen, H. Y.; Lee, F. S.; Yang, M. H. Polym Test 2003, 22, 31.